Identification of bulk and surface sulfur impurities in Ti O 2 by synchrotron x-ray absorption near edge structure

M. F. Smith, Kongthip Setwong, Rungnapa Tongpool, Darin Onkaw, Sutassana Na-phattalung, Sukit Limpijumnong, and Saroj Rujirawat

Citation: Applied Physics Letters **91**, 142107 (2007); doi: 10.1063/1.2793627
View online: http://dx.doi.org/10.1063/1.2793627
View Table of Contents: http://scitation.aip.org/content/aip/journal/apl/91/14?ver=pdfcov
Published by the AIP Publishing

Identification of bulk and surface sulfur impurities in TiO_2 by synchrotron x-ray absorption near edge structure

M. F. Smith[a),b)]
National Synchrotron Research Center, Nakhon Ratchasima 30000, Thailand

Kongthip Setwong and Rungnapa Tongpool
National Metal and Materials Technology Center, Pathumthani 12120, Thailand

Darin Onkaw, Sutassana Na-phattalung, Sukit Limpijumnong, and Saroj Rujirawat[a)]
School of Physics, Suranaree University of Technology, Nakhon Ratchasima 30000, Thailand and National Synchrotron Research Center, Nakhon Ratchasima 30000, Thailand

(Received 26 July 2007; accepted 12 September 2007; published online 3 October 2007)

Synchrotron x-ray absorption near edge structure (XANES) measurements of Ti and S *K* edges, combined with first principles simulations, are used to characterize S-doped TiO_2 prepared by oxidative annealing of TiS_2 at various temperatures. Ti-edge XANES and x-ray powder diffraction data indicate that samples annealed above 300 °C have an anatase TiO_2 crystal structure with no trace of TiS_2 domains. S-edge XANES data reveal that the local structure seen by S atoms evolves gradually, from TiS_2 to a qualitatively different structure, as the annealing temperature is increased from 200 to 500 °C. For samples annealed at 500 °C, the spectrum appears to have features that can be assigned to S on the surface in the form of SO_4 and S defects in the bulk (most likely S interstitials) of TiO_2. © *2007 American Institute of Physics*. [DOI: 10.1063/1.2793627]

TiO_2 is a semiconductor photocatalyst which is used in applications such as air and water purifications.[1–3] Despite its advantages over other materials, such as better oxidizing power and chemical stability, its applicability is limited by a band gap (3.0–3.2 eV) that is too large to utilize effectively the spectrum of sunlight. A longstanding challenge is to lower the band gap of the material without too severely compromising properties beneficial to photocatalysis.

Sulfur-doped TiO_2, prepared by oxidative annealing of TiS_2, has been found to have a lower band gap than pure TiO_2, giving a higher photocurrent under visible light.[4,5] Enhanced photocatalysis is seen when TiO_2 is doped with some elements, such as C, N, and F, which are claimed to substitute for O in the bulk, and S doping may have similar effects.[6–11] On the other hand, S impurities are known to inhibit photocatalytic reactions, so unwanted S impurities might limit photocatalytic performance.[12–14] To understand the role of sulfur in photocatalysis, it would be helpful to know how S is incorporated into TiO_2.

Here, sulfur-doped TiO_2 prepared by oxidative annealing of TiS_2 powder[4] is characterized by Ti and S *K*-edge x-ray absorption near edge structue (XANES) measurements. Samples were annealed in air at 200, 300, 400, or 500 °C for 2 h. XANES measurements were made in the transmission mode at the X-ray absorption spectroscopy beamline (BL-8) of the Siam photon source (electron energy of 1.2 GeV), National Synchrotron Research Center (Thailand). Crystal monochromators [Si (111) for Ti *K* edge and InSb(111) for S *K* edge] were used with a scanning energy step of 0.25 eV. For energy calibration of Ti and S edges, we compared our XANES measurements of TiO_2 and TiS_2, respectively, to previously published spectra.[15,16] X-ray powder diffraction (XRD) measurements were made for each sample to verify the crystal structure. More details of the sample preparation and measurement will be published elsewhere.[17] The measured Ti and S *K*-edge XANES spectra are shown in Fig. 1 in comparison with the spectra for pure TiO_2 and TiS_2.

The Ti *K*-edge XANES of the sample annealed at 200 °C combines features of TiS_2 and TiO_2, indicating that oxidation is not completed and there are surviving TiS_2 domains at this temperature (Fig. 1, left panel). For samples annealed at 300 °C and above, the spectra are indistinguishable from that of pure TiO_2, suggesting a full conversion to TiO_2. Since the number of S atoms in such annealed samples is small compared to the number of O atoms, the Ti *K*-edge XANES will be little affected by the small fraction of Ti that lie close to S impurities. The XRD measurements (not shown) are consistent with these results; i.e., they indicate a small amount of TiS_2 in the sample annealed at 200 °C and no detectable TiS_2 domain for samples that are annealed at 300 °C and above. The TiO_2 structure is largely anatase, with a small (roughly 5%) rutile admixture.

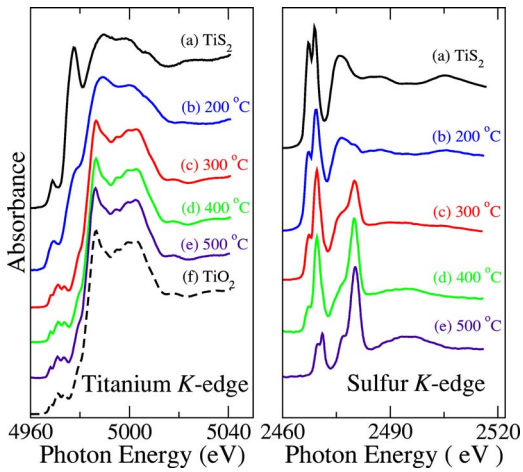

FIG. 1. (Color online) Measured Ti (left panel) and S (right panel) *K*-edge XANESs. Curve (a) is for pure (unannealed) TiS_2 sample, while curves (b)–(e) are for TiS_2 that has been annealed in air for 2 h at temperatures of 200, 300, 400, and 500 °C, respectively. The spectrum of a pure TiO_2 is shown with a dashed curve (f).

a)Authors to whom correspondence should be addressed.
b)Current address. Department of Physics, University of Queensland, 4072 Brisbane, Australia. Electronic mail: msmith@physics.utoronto.ca

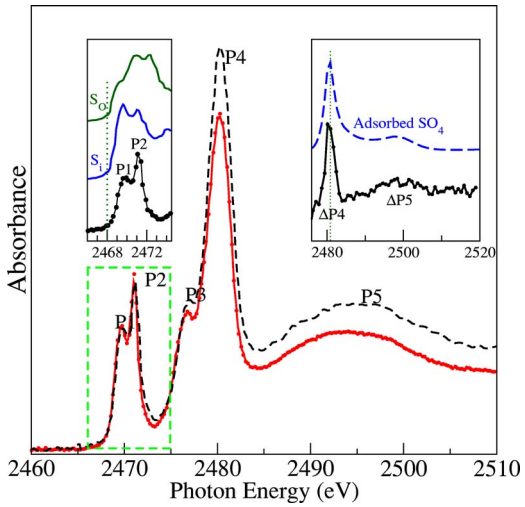

FIG. 2. (Color online) Sulfur *K*-edge XANES of the 500 °C annealed sample before (dashed curve) and after (solid curve) being washed with water. The lower-energy features (peaks P1 and P2), corresponds to S in the bulk, while the features in the higher-energy region (P3–P5) correspond to S at the TiO_2 surface. Left inset: comparison between the measured XANES in the lower-energy region (bottom curve) with the simulation for bulk S defects (from top: S_O and S_i) in TiO_2. The difference between the spectrum befre and after washing is compared to the simulated XANES of S on TiO_2 surface in the form of SO_4. The absolute photon energy of simulated spectra was slightly shifted (all shifts are smaller than 3 eV) to align a particular feature with the measured spectra.

Information on the local structure surrounding the remaining S atoms can be revealed by analyzing S *K*-edge XANES data (Fig. 1, right panel). At 200 °C, the XANES features remain similar to those of TiS_2, indicating that the local structure surrounding S atoms is TiS_2. With increasing temperature, new features emerge while TiS_2 features are reduced such that the spectrum for samples annealed at 500 °C is qualitatively different from TiS_2. For the 500 °C annealed sample, XANES features can be divided into two regions (Fig. 2). In the lower-energy region, there are asymmetric double peaks, P1 (near 2469 eV) and P2 (2471 eV). In the higher-energy region, features are broader and include a large peak P4 (2481 eV), preceded by a small peak P3 (2477 eV), and followed by a broad hump P5 (centered on 2494 eV).

To interpret the observed XANES features, we use first principles simulations of XANES for S at various locations within anatase TiO_2, including bulk and surface sites. The simulations were performed using the FEFF 8 code[18] which employs a full-multiple scattering approach from self-consistent overlapping muffin-tin atomic potentials. The cluster size was increased until spectra converged (40–80 atoms, depending on the defect). From the simulations of pure systems such as TiS_2 and free SO_4 molecule, we found that the XANES features are in good agreement with the known spectra. However, the simulated absolute photon energies differed from the measured values by 1–2 eV (the relative energies are much more accurate).

For bulk defects, we have calculated sulfur substitute oxygen (S_O), sulfur substitute titanium (S_{Ti}), and sulfur interstitial (S_i). To achieve realistic local atomic structures surrounding the S atom and to gain insight into the impurity (electronic) levels, each bulk defect was initially studied by a *first principles* total energy calculation based on the Vienna *ab initio* Simulation Package (VASP 4.6) using the supercell approach.[19] The electron distributions and the position of each atom are allowed to relax to their minimum energy configurations in the calculations (all Hellman-Feynman forces in our 48–atom supercell are less than 0.05 eV/Å in the relaxed structure.) We used density functional theory within the local density approximation and ultrasoft pseudopotentials. The cutoff energy for the plane-wave basis set is 300 eV. (The details of the computations are similar to those in Ref. 20.) All three impurities are found to produce defect levels in the TiO_2 band gap. As a result, the stable charge state of the impurities changes from being positive (2+ for S_O and S_{Ti} and 4+ for S_i) to neutral as the Fermi level is raised through the defect levels. (Note that one should not confuse "charge state" with "oxidation number." They are different quantities.) We carried out the XANES simulations for both stable charge states for each bulk impurity configuration.

The bulk defect spectra have at least one thing in common: their main peaks are located in the photon energy range of 2465–2475 eV (i.e., within the lower-energy region of the measured spectrum). Therefore, while bulk defects may explain the lower-energy region, they cannot be responsible for features observed in the higher-energy region. We compare all the bulk defect spectra to the observed lower-energy region to identify the most likely bulk S site.

The simulated spectra of S_{Ti} (not shown) do not resemble the data and are therefore excluded. The simulations of S_O and S_i are shown in comparison with the measured XANES (Fig. 2, left inset). For ease of comparison, each simulation is shifted in energy so that its absorption threshold is aligned with the measured value (shifted down by 1.5–1.9 eV), and only the charge state most resembling the data for each defect is shown. The simulated spectrum of S_i is a closer match to the observed spectrum than that of S_O. The simulation for the neutral S_i accounts for (1) the relative position of P1 (1.6 eV above the threshold) and (2) the P2-P1 peak separation (1.4 eV). Although S_O cannot be completely ruled out, we tentatively assign the P1-P2 double peak feature observed in the lower-energy region to interstitial sulfur. This assignment is supported by the fact that the anatase phase of TiO_2 has ample interstitial space and our previous total energy calculations have shown interstitial defects to be favorable for many nonmetallic species, especially in O-rich growing conditions. The local structure of neutral S_i obtained from our first principles structural relaxation is illustrated in Fig. 3. The interstitial S atom bonds strongly with one of the lattice O, forming a split-interstitial configuration with S–O bond distance of 1.8 Å. The next nearest neighbors of the S atom are an O at 2.2 Å and three Ti at 2.3–2.4 Å, arranged asymmetrically.

Since none of the bulk defects can be responsible for the high-energy peaks (P3–P5), we consider surface sulfur impurities. The center of the main peak (P4) of 2480 eV is near that identified as surface SO_x.[21] Surface SO_x species are thus potential candidates. (Moreover, previous measurements have indicated SO_x species, with $x=2,3,4$, on TiO_2 sample surfaces.[22]) For simplicity, we use an ideal bulk-truncated structure of the (101) surface, which is known to be the most stable surface.[2] SO_x species were positioned near the surface and their absorption spectra simulated.

Surface SO_x (with $x=2,3,4$) species are studied. (SO on the surface was also considered but found to be inconsistent with the data.) Considered arrangements included those with

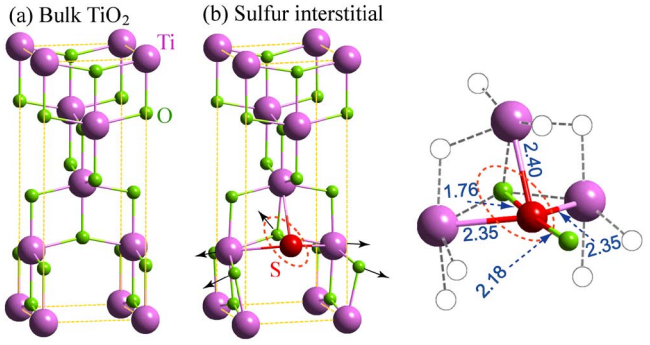

FIG. 3. (Color online) Atomic structures of (a) bulk anatase TiO_2 and (b) sulfur interstitial (S_i) with a zoom view of the latter on the far right. The large, medium, and small spheres are Ti, S, and O atoms, respectively. The dashed ellipse indicates the split-interstitial S–O pair. The arrows show the relaxation of the neighboring atoms compared to their positions in the bulk. In the zoom, the bond distances from S to its neighbors are given in angstroms and an additional O, from an adjacent unit cell, appears.

an O in the SO_x binding to a fivefold coordinated Ti atom (in the next-to-top layer) and those with a twofold coordinated O atom (surface O of TiO_2) included in the SO_x. For the former, the displacement of the molecule from the surface was also varied (see Ref. 23) In general, the spectrum of SO_2 was sensitive to such variations, while the SO_3 and SO_4 spectra were not. There was little qualitative surface-orientation dependence, as judged by test calculations using (101) and (001) surfaces.

The spectra of SO_2 and SO_3 species have strong absorption peaks located close to 2470 eV (near P1 and P2), and second peaks close to 2480 eV (near P4), whereas the spectrum of SO_4 species shows only the latter. However, only SO_3 and SO_4 spectra show a feature that corresponds well with the position and shape of P5. This makes the latter two species of surface sulfur the most promising candidates. After considering the observed effect of washing the samples (described next), the SO_4 species emerge as that most likely responsible for P4 and P5.

To test the stability of S in the sample, the (500 °C) sample was washed with distilled water. The measured XANESs before (dashed line) and after (solid line) washing are shown in Fig. 2. The spectra are normalized by matching the heights of corresponding P1. While the position and shape of features appear unchanged, there is a clear reduction of P3–P5 upon washing, which suggests that some S absorbers are washed away. These data cannot be easily explained if the SO_3 species on the surface are primarily responsible for the high-energy peaks. For, if it were, then SO_3 would contribute significantly to the lower-energy region as well. This would make it difficult to explain the large change in high-energy absorption relative to low-energy absorption that is produced by washing. Furthermore, SO_3 is not likely to contribute much to the lower-energy region since the latter is much better described by the bulk S interstitial simulation discussed above.

To study the sulfur species that is washed away, we plot the difference between unwashed and washed XANES spectra (Fig. 2, right inset). The spectrum of this difference is dominated by peaks corresponding to P4 and P5 and is in good agreement with the simulated spectrum of the surface SO_4 apecies considered (dashed line). Note that, for ease of comparison, the simulation was shifted (up by about 2 eV) to align its main peak with that of the measurement. This suggests that surface S in SO_4 form is largely responsible for the washing dependence of the spectra and thus for the high-energy peaks in annealed samples.

In summary, we have studied Ti and S *K*-edge XANESs of sulfur-doped TiO_2 prepared by oxidative annealing of TiS_2. For annealing temperatures of 300 °C or above, the samples are converted to TiO_2 with no detectable TiS_2 phase, according both to XRD and Ti-edge XANES measurements. The S-edge XANES spectrum is found to gradually evolve away from that of TiS_2, developing new qualitative features, as the annealing temperature is increased from 200 to 500 °C. The XANES spectrum of the high (500 °C) annealing-temperature sample, in conjunction with first principles calculations, indicates that sulfur atoms are mainly on the TiO_2 surface as SO_4 and, within the sample, most likely in the form of split interstitials (S_i). The detailed description of surface and bulk incorporation of S in TiO_2 provided by XANES measurements here will be useful for disentangling various influences on photocatalysis in sulfur-doped TiO_2.

This work is partially supported by MTEC (Grant No. MT-B-49-CER-07-195-I) and Commission on Higher Education, Thailand (CHE-RES-RG "Theoretical Physics").

[1]M. R. Hoffmann, S. T. Martin, W. Choi, and D. H. Bahnemann, Chem. Rev. (Washington, D.C.) **95**, 69 (1995).
[2]U. Diebold, Surf. Sci. Rep. **48**, 53 (2003).
[3]K. Hashimoto, H. Irie, and A. Fujishima, Jpn. J. Appl. Phys., Part 1 **44**, 8269 (2005).
[4]T. Umebayashi, T. Yamaki, H. Itoh, and K. Asao, Appl. Phys. Lett. **81**, 454 (2002).
[5]T. Umbeyashi, T. Yamaki, S. Yamamoto, A. Miyashita, S. Tanaka, T. Sumita, and K. Asai, J. Appl. Phys. **93**, 5156 (2003).
[6]S. U. M. Khan, M. Al-Shahry, M. Al-Shahry, and W. B. Ingler, Science **297**, 2243 (2002).
[7]H. Wang and J. P. Lewis, J. Phys.: Condens. Matter **17**, L209 (2005).
[8]C. Di Valentin, G. Pacchioni, and A. Selloni, Phys. Rev. B **70**, 085116 (2004).
[9]H. Wang and J. P. Lewis, J. Phys.: Condens. Matter **18**, 421 (2006).
[10]R. Asahi, T. Morikawa, T. Ohwaki, A. Aoki, and Y. Taga, Science **293**, 269 (2001).
[11]A. Hattori, M. Yamamoto, H. Tada, and S. Ito, Chem. Lett. **8**, 707 (1998).
[12]E. L. Hebenstreit, W. Hebenstreit, and U. Diebold, Surf. Sci. **461**, 87 (2000).
[13]J. A. Rodriguez, S. Chaturvedi, M. Kuhn, and J. Hrbek, J. Phys. Chem. B **102**, 5511 (1998).
[14]J. A. Rodriguez and J. Hrbek, Acc. Chem. Res. **32**, 719 (1999).
[15]F. Farges, G. E. Brown, Jr., and J. J. Rehr, Phys. Rev. B **56**, 1809 (1997).
[16]Z. Y. Wu, F. Lemoigno, P. Gressier, G. Ouvrard, P. Moreau, J. Rouxel, and C. R. Natoli, Phys. Rev. B **54**, R1109 (1996).
[17]D. Onkaw (unpublished).
[18]A. L. Ankudinov, B. Ravel, J. J. Rehr, and S. D. Conradson, Phys. Rev. B **58**, 7565 (1998).
[19]G. Kresse and J. Furthmüller, Comput. Mater. Sci. **6**, 15 (1996).
[20]S. Na-Phattalung, M. F. Smith, K. Kim, M.-H. Du, S.-H. Wei, S. B. Zhang, and S. Limpijumnong, Phys. Rev. B **73**, 125205 (2006).
[21]J. A. Rodriguez, T. Jirsak, S. Chaturvedi, and M. Kuhn, Surf. Sci. **442**, 400 (1999).
[22]D. I. Sayago, P. Serrano, O. Böhme, A. Goldoni, G. Paolucci, E. Román, and J. A. Martin-Gago, Phys. Rev. B **64**, 205402 (2001).
[23]Note that first principles surface structural relaxations were not performed, so the actual local structure surrounding surface S defects was not determined. Rather, we considerd several simplified surface defect configurations and simulated their XANES spectra to determine which, if any, is consistent with the high-energy features of the data.